Journal of Engineering Mathematics 19 (1985) 217–231.

Exact solutions for the probability density function of turbulent scalar fields

R. KOWE [1] and P.C. CHATWIN [2,*]

[1] *Physiological Flow Studies Unit, Imperial College, London SW7, UK,* [2] *Department of Applied Mathematics and Theoretical Physics, University of Liverpool, P.O. Box 147, Liverpool L69 3BX, UK*

(Received March 22, 1985)

Summary

The basic property of a turbulent scalar field is its probability density function $p(\theta; x, t)$. Here, for the first time, some exact solutions for $p(\theta; x, t)$ are derived and discussed. These apply to the case of a finite mass of passive scalar – called a cloud for short – dispersing in simple, but conceptually important, turbulent flows, namely those associated with constant rates of strain. Extensions of the solutions to cases where the cloud is meandering, and where there are several clouds, are obtained. Applications of the results are discussed, with particular emphasis on their potential value for testing and validating approximate closure schemes applied to the evolution equation for $p(\theta; x, t)$.

1. Introduction

It is now widely recognized that there are many engineering problems involving turbulent diffusion phenomena whose satisfactory practical resolution requires more knowledge than simply that of the variation with position x and time t of $C(x, t)$, the (ensemble) mean concentration of the dispersing scalar. This is particularly true, perhaps, of any situation where the assessment of hazards is involved. For example, Birch, Brown and Dodson [1] demonstrated very poor correlation between the mean concentration in a methane jet and the probability that ignitable conditions exist, and Ride [2,3] has emphasized the crucial importance in toxicity assessment of fluctuations in the scalar concentration about its mean.

Such recognition of the inadequacy of conventional methods in many situations has generated an upsurge of research interest in the behaviour of these fluctuations. Let $\Gamma(x, t)$ be the concentration (in arbitrary units) of the dispersing scalar in any one realization of an ensemble of releases. The central importance of the concept of an ensemble has been emphasized elsewhere [4] and is basic to all that follows. Since the scalar is being dispersed in a turbulent flow, $\Gamma(x, t)$ is a random variable with a probability density function (p.d.f.) $p(\theta; x, t)$ such that

$$p(\theta; x, t)\delta\theta = P(\theta \leqslant \Gamma(x, t) < \theta + \delta\theta) \tag{1}$$

* Present address: Department of Mathematics and Statistics, Brunel University, Uxbridge, Middlesex UB8 3PH, UK.

where the symbol P stands for "the probability that". Thus, for example, when θ_1 and θ_2 are the stoichiometric limits for a flammable gas,

$$\int_{\theta_1}^{\theta_2} p(\theta;\, x,\, t)\mathrm{d}\theta = P(\theta_1 \leqslant \Gamma(x,\, t) \leqslant \theta_2) \tag{2}$$

is the probability that ignitable conditions exist at position x and time t. It is obvious that

$$\int_0^\infty p(\theta;\, x,\, t)\mathrm{d}\theta = 1 \tag{3}$$

and, in statistical parlance, the mean concentration $C(x,\, t)$ and the mean square fluctuation $\overline{c^2}(x,\, t)$ are, respectively, the mean and variance of $\Gamma(x,\, t)$. Thus

$$C(x,\, t) = \int_0^\infty \theta p(\theta;\, x,\, t)\mathrm{d}\theta; \quad \overline{c^2}(x,\, t) = \int_0^\infty (\theta - C)^2 p(\theta;\, x,\, t)\mathrm{d}\theta. \tag{4}$$

It needs noting that, in practice, there will be a maximum attainable concentration $\theta_{\max}$ (e.g. the initial scalar concentration) and a minimum attainable concentration $\theta_{\min}$ (which will often be zero). Thus the limits 0 and ∞ in (3) and (4) can be replaced by $\theta_{\min}$ and $\theta_{\max}$ respectively; but, since p must be identically zero for $0 \leqslant \theta < \theta_{\min}$ and for $\theta > \theta_{\max}$, such replacement is unnecessary.

The single most important statistical property describing fluctuations about the mean is $\overline{c^2}(x,\, t)$ and much research, both experimental (e.g. [5], [6], [7], [8], [9]) and theoretical (e.g. [10], [11]) has been devoted to it. But knowledge about $\overline{c^2}$ is inadequate for many practical problems, and for complete scientific understanding, unless the form of $p(\theta;\, x,\, t)$ is also known and, furthermore, is completely specified by the values of C and $\overline{c^2}$ as functions of x and t. As shown by measurements in [1] and elsewhere (e.g. [12], [13], [14]) however, real flows are not (unfortunately!) associated with p.d.f.s with such simple properties; in particular the functional dependence of p on θ varies strongly with x. Further theoretical research on the p.d.f. is therefore highly desirable.

Such research as has already been published has begun with the evolution equation for $p(\theta;\, x,\, t)$ which, for constant-density incompressible flow, can be written ([15], [16])

$$\frac{\partial p}{\partial t} + \boldsymbol{U}\cdot\nabla p + \nabla\cdot\left\{\overline{\boldsymbol{u}\delta[\Gamma(x,\, t)-\theta]}\right\}$$

$$= \kappa\nabla^2 p - \kappa\frac{\partial^2}{\partial\theta^2}\left\{\overline{(\nabla\Gamma)^2\delta[\Gamma(x,\, t)-\theta]}\right\}, \tag{5}$$

where overbars denote ensemble means, κ is the molecular diffusivity, and $\boldsymbol{U} = \boldsymbol{U}(x,\, t)$, $\boldsymbol{u} = \boldsymbol{u}(x,\, t)$ are, respectively, the mean and fluctuation in the velocity field. Like all equations for statistical properties of turbulent fields, equation (5) exhibits the closure problem. In this case the last terms on each side of the equation are not expressible exactly in terms of p. Progress can therefore be made from equation (5) only if these terms can be approximated by expressions involving p; such approximations are called closure hypotheses and are inevitably empirical (and almost certainly incorrect – in a strict sense – given the present state of the art). Pope [16] gives a critical discussion of the closure hypotheses that have been applied to equation (5).

2. The basis of the presente work

Many important papers on turbulence and turbulent diffusion have used exact solutions for a situation when the instantaneous velocity field $\mathcal{V}(x, t)$ is linear in the coordinates of x. While this idealized flow is applicable to real turbulent flows only when discussing relative motion over scales no greater than a few multiples of the Kolmogoroff microscale, results derived for it have proved extremely enlightening. Saffman [17] gave the general solution for a scalar field dispersing in such a flow. Here, to avoid great algebraic complications which add little to the ideas, only the special solution first given by Townsend [18] will be used. Chatwin and Sullivan [10] used this solution in discussing the structure of $\overline{c^2}(x, t)$ associated with a dispersing cloud of scalar contaminant.

Within the neighbourhood of any moving fluid particle, the velocity field relative to that of this particle is composed of a solid-body rotation and a uniform strain, and the turbulent motion is statistically isotropic. When the initial distribution of the scalar concentration $\Gamma(x, t)$ has spherical symmetry about the moving fluid particle, the solid body rotation has no effect on the statistical properties of $\Gamma(x, t)$, including $p(\theta; x, t)$. It is therefore sufficient to take axes coinciding with the instantaneous principal axes of the rate of strain tensor so that the velocity field $\mathcal{V}(x, t)$ takes the form

$$\mathcal{V} = (\alpha_1 x_1, \alpha_2 x_2, \alpha_3 x_3), \tag{6}$$

where

$$\alpha_1 + \alpha_2 + \alpha_3 = 0 \tag{7}$$

to satisfy incompressibility. The values of the principal rates of strain α_i $(i = 1, 2, 3)$ are of order $(\epsilon/\nu)^{1/2}$ in standard notation, and their magnitudes change relatively slowly with t so that they will be supposed constant in what follows. However, as shown by Townsend [18], the solution given below can easily be amended when the rates of strain vary with time, and these amendments cause no significant change to the results presented here for $p(\theta; x, t)$. With the velocity field given by (6), the equation governing $\Gamma(x, t)$ is

$$\frac{\partial \Gamma}{\partial t} + \alpha_1 x_1 \frac{\partial \Gamma}{\partial x_1} + \alpha_2 x_2 \frac{\partial \Gamma}{\partial x_2} + \alpha_3 x_3 \frac{\partial \Gamma}{\partial x_3} = \kappa \left(\frac{\partial^2 \Gamma}{\partial x_1^2} + \frac{\partial^2 \Gamma}{\partial x_2^2} + \frac{\partial^2 \Gamma}{\partial x_3^2} \right), \tag{8}$$

with appropriate boundary and initial conditions.

Here it will be supposed that there are no boundaries; thus

$$\Gamma(x, t) \to 0 \qquad \text{as} \quad |x| \to \infty. \tag{9}$$

The most important initial conditions in practice are those in which there is a finite quantity Q of scalar, since other situations such as a continuous source can then be dealt with by superposition. The case when the scalar is distributed uniformly within a sphere is considered by Kowe [19] and, more briefly, in [20]. The solution of Townsend [18] is algebraically more convenient (since there are no singularities) and has

$$\Gamma(x, 0) = \frac{2^{3/2} Q}{L_0^3} \exp\left\{ - \frac{2\pi |x|^2}{L_0^2} \right\}, \tag{10}$$

where L_0 is a constant, characteristic of the initial spatial extent of the scalar cloud. The solution of (8), satisfying (9) and (10). was given in [18] and is

$$\Gamma(x, t) = \frac{2^{3/2}Q}{L_1 L_2 L_3} \exp\left\{-2\pi\left(\frac{x_1^2}{L_1^2} + \frac{x_2^2}{L_2^2} + \frac{x_3^2}{L_3^2}\right)\right\}, \tag{11}$$

where the $L_i = L_i(t)$ $(i = 1, 2, 3)$ are given by

$$L_i^2 = \left(L_0^2 + \frac{4\pi\kappa}{\alpha_i}\right) \exp(2\alpha_i t) - \frac{4\pi\kappa}{\alpha_i}. \tag{12}$$

With this solution, the surfaces of constant scalar concentration are ellipsoids with semi-major axes L_1, L_2, L_3. From (7) it is obvious that at least one of the α_i is positive and at least one is negative. According to (12), the value of L_i when α_i is positive increases with t, whereas that for a negative α_i approaches $(4\pi\kappa/|\alpha_i|)^{1/2}$ which is of order $(\nu\kappa^2/\epsilon)^{1/4}$ – the conduction cut-off length. Thus, qualitatively, there are two possibilities. When two of the α_i are positive the ellipsoids tend to become sheets of constant thickness and increasing area ("discuses"); when two of the α_i are negative the ellipsoids tend to become threads of constant cross-sectional area but increasing length ("cigars").

3. Some simple models for the p.d.f.

As noted earlier, the p.d.f. $p(\theta; x, t)$ can be defined only in relation to a specified ensemble of releases, and it is now necessary to consider possible ensembles involving the exact solution (11). At any point the directions of the principal axes of the rate of strain tensor are oriented randomly in space, and the simplest possible ensemble consists of a series of releases differing only in this orientation, which has an assigned probability distribution. In all other respects each release is identical, and, in each, the scalar concentration is given by (11) with respect to the appropriate axes for that release.

Since the fine-scale structure of most turbulent flows is isotropic, it is natural first to consider the case where all orientations are equiprobable. Consider a point distance $r = |x|$ from the origin, and suppose for the moment (without loss of generality) that $\alpha_1 \ll \alpha_2 \ll \alpha_3$ so that $L_1 \ll L_2 \ll L_3$. Then it is evident from (11) that, at this point, the perceived concentration is bounded below by $\theta_{\min}$ and above by $\theta_{\max}$, where

$$\theta_{\min} = A \exp\left(-\frac{2\pi r^2}{L_1^2}\right), \quad \theta_{\max} = A \exp\left(-\frac{2\pi r^2}{L_3^2}\right), \tag{13}$$

with $A = A(t)$ given by

$$A(t) = 2^{3/2}Q/(L_1 L_2 L_3). \tag{14}$$

It is also evident geometrically, as shown schematically in Fig. 1, that the p.d.f. of the concentration can be obtained for this particular case of isotropy by considering the variation of concentration on a sphere with the distribution of concentration fixed in space. Indeed, suppose $\mathbb{P}(\theta; x, t)$ is the cumulative distribution function (c.d.f.) so that

$$\mathbb{P}(\theta; x, t) = P(\Gamma(x, t) \leqslant \theta). \tag{15}$$

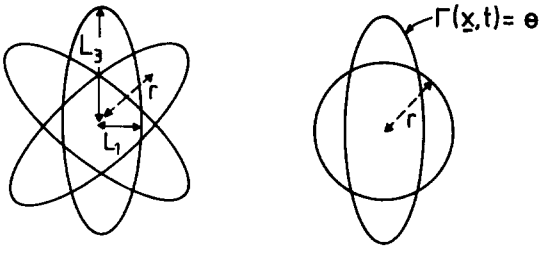

Figure 1. Sketch illustrating the text discussion of the form of p for a point at a distance $r = |x|$ from the centre of an ellipsoid, the direction of whose principal axes are orientated randomly in space with an isotropic distribution.

Then, in the present case, $\mathbb{P}(\theta;\ x,\ t) = \mathbb{P}(\theta;\ r,\ t)$ is the proportion of the surface area of a sphere of radius r lying outside that ellipsoid on which $\Gamma = \theta$, where $\Gamma = \Gamma(x,\ t)$ is given by (11) and θ is any concentration between $\theta_{\min}$ and $\theta_{\max}$. The p.d.f. $p(\theta;\ x,\ t)$ is then of course given by the general formula

$$p(\theta;\ x,\ t) = \frac{\partial}{\partial\theta}\mathbb{P}(\theta;\ x, t). \tag{16}$$

Even for this simplest case the algebraic details are complicated when L_1, L_2, L_3 are all different. There are, fortunately, two special cases which are very typical and illustrate the method. These occur when two of the α_i–and hence two of the L_i–are equal. Suppose first that $\alpha_1 < 0$ and that $\alpha_2 = \alpha_3 > 0$, so that the surfaces $\Gamma = \theta$ tend to become sheets in the shape of discuses. Writing $x_1 = r\cos\psi$, $x_2 = r\sin\psi\cos\phi$, $x_3 = r\sin\psi\sin\phi$ gives $\Gamma = \theta$ when $\psi = \psi_0$, where (remembering that $L_2 = L_3$)

$$\cos^2\psi_0 = \frac{L_3^2 L_1^2}{L_3^2 - L_1^2}\left\{\frac{\ln(A/\theta)}{2\pi r^2} - \frac{1}{L_3^2}\right\} \qquad \text{for} \quad \theta_{\min} \leqslant \theta \leqslant \theta_{\max}. \tag{17}$$

Hence

$$\mathbb{P}(\theta;\ x,\ t) = \begin{cases} 1 & \text{for} \quad \theta \geqslant \theta_{\max}; \\ 1 - \cos\psi_0 & \text{for} \quad \theta_{\min} \leqslant \theta \leqslant \theta_{\max}; \\ 0 & \text{for} \quad \theta \leqslant \theta_{\min}. \end{cases} \tag{18}$$

Thus, using (16),

$$p(\theta;\ r,\ t) = \begin{cases} \dfrac{L_1 L_3}{(8\pi)^{1/2} r\theta}\left\{\left(L_3^2 - L_1^2\right)\left[\ln\left(\dfrac{A}{\theta}\right) - \dfrac{2\pi r^2}{L_3^2}\right]\right\}^{-1/2} \\ \quad \text{for} \quad \theta_{\min} < \theta < \theta_{\max}; \\ 0 \qquad \text{for} \quad \theta < \theta_{\min} \text{ and } \theta > \theta_{\max}. \end{cases} \tag{19}$$

The dependence of p on r is shown explicitly in (19), while that on t is contained in the expressions for L_1, L_3 and A given in (12) and (14). It is however remarkable that there

are rescaled variables in terms of which (19) has a self-similar form. Thus define Θ and $\Theta_{\min}$ by

$$\Theta = \frac{\theta}{\theta_{\max}}, \quad \Theta_{\min} = \frac{\theta_{\min}}{\theta_{\max}}, \tag{20}$$

where $\theta_{\min}$ and $\theta_{\max}$ are defined in (13). Simple manipulation then gives

$$\theta_{\max} p(\theta; r, t) = \begin{cases} \left(\frac{1}{2\Theta}\right)\{(\ln \Theta)(\ln \Theta_{\min})\}^{-1/2} & \text{for} \quad \Theta_{\min} \leqslant \Theta < 1; \\ 0 \quad \text{for} \quad \Theta < \Theta_{\min} \text{ and } \Theta > 1. \end{cases} \tag{21}$$

The other special case occurs when $\alpha_1 > 0$ and $\alpha_2 = \alpha_3 < 0$; in this case the surfaces $\Gamma = \theta$ tend to become threads in the shape of cigars. The calculation of p can be carried out in an analogous manner to that for discuses just illustrated. The result corresponding to (21) is

$$\theta_{\max} p(\theta; r, t) = \begin{cases} \left(\frac{1}{2\Theta}\right)\{(\ln[\Theta_{\min}/\Theta])(\ln \Theta_{\min})\}^{-1/2} \\ \quad \text{for} \quad \Theta_{\min} < \Theta \leqslant 1; \\ 0 \quad \text{for} \quad \Theta < \Theta_{\min} \text{ and } \Theta > 1. \end{cases} \tag{22}$$

The results in (21) and (22) are shown in Fig. 2. Several points are worth making. Neither curve has anything like the behaviour of p.d.f.s, such as the Normal p.d.f., commonly encountered in other fields, and there are singularities at the end-points where $\Theta = \Theta_{\min}$ and $\Theta = 1$, even though the effects of molecular diffusion are fully included. For the

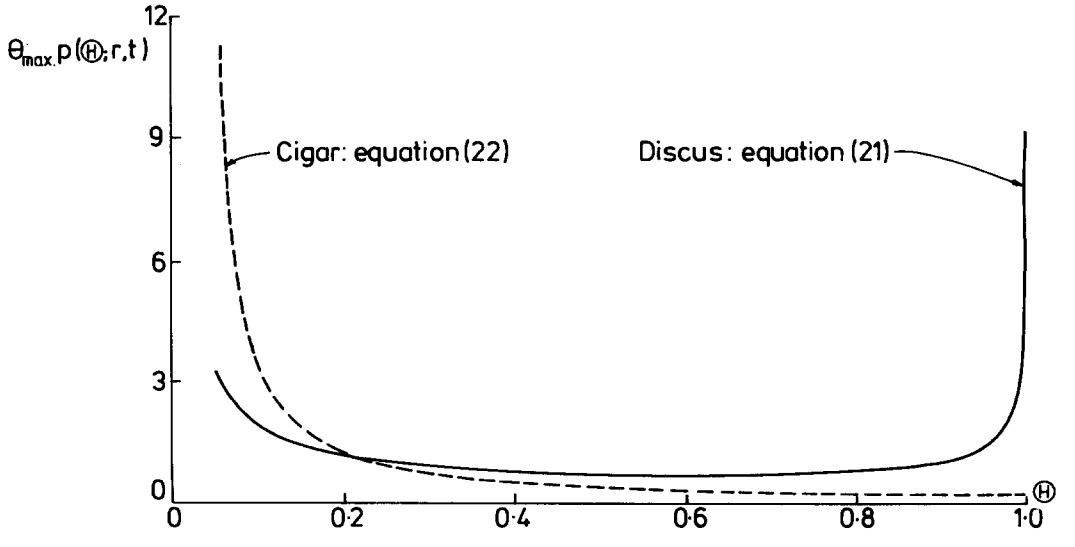

Figure 2. Non-dimensionalised form of the p.d.f. $p(\Theta; r, t)$ for the discus and cigar, given by equations (21) and (22) respectively. In this figure $\Theta_{\min} = 0.01$.

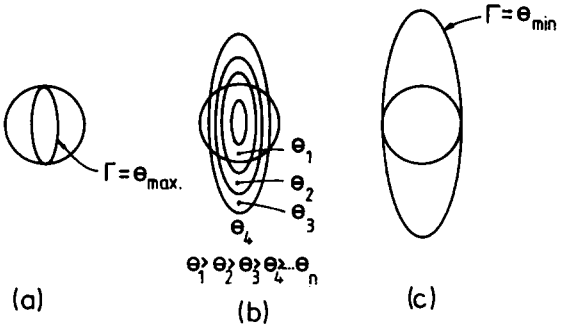

Figure 3. Sketch showing a sphere radius r intersecting a set of ellipsoids on which the concentration ranges from (a) θ_{max} to (c) θ_{min}. Figure (b) shows how concentration varies with size of ellipsoid.

discus, p has an infinite spike at $\Theta = 1$ because, for this concentration, the sphere and discus intersect in a circle of radius L_3; see Fig. 3(a). Conversely there is no spike at $\Theta = 1$ for the cigar since the intersection is only the end-point of a line. At $\Theta = \Theta_{min}$, the situation is reversed as shown in Fig. 3(c). It is worth noting that for the discus there is a finite spike near Θ_{min} although the intersection is also at the ends of a line. The radius of curvature however is smaller at these points than for the cigar and this has a significant effect.

Results like (21) and (22) hold for ensembles in which the orientations of the principal axes are distributed isotropically. Another ensemble of interest is that when the axes are distributed axisymmetrically, which is the situation found, for example, in a jet flow. Consider, for simplicity, the two-dimensional shear field $\mathcal{T} = (\alpha_1 x_1, \alpha_2 x_2)$ (so that $\alpha_1 + \alpha_2 = 0$) where $x_1 = r\cos\psi$, $x_2 = r\sin\psi$. With the initial distribution

$$\Gamma(x, 0) = \frac{2Q}{L_0^2}\exp\left(-\frac{2\pi r^2}{L_0^2}\right), \tag{23}$$

the solution of equation (18) (ignoring the variation in the x_3 component) is given by

$$\Gamma(x, t) = A\exp\left\{-2\pi\left(\frac{x_1^2}{L_1^2} + \frac{x_2^2}{L_2^2}\right)\right\}, \tag{24}$$

where the $L_i(t)$ are given by equation (12) and $A(t) = 2Q/(L_1 L_2)$. Equation (24) implies that *curves* of constant Γ are ellipses. Taking $\alpha_2 = -\alpha_1 > 0$, which gives an ellipse with semimajor axis L_2, it follows that $\Gamma = \theta$ when $\psi = \psi_0$, where ψ_0 is defined by equation (17) replacing L_3 with L_2.

We now choose a suitable distribution $p(\beta)$ for β, the angle of the axis L_2 to a fixed direction in the flow, as illustrated in Fig. 4. A simple axisymmetric distribution is the circular distribution

$$p(\beta) = \frac{1}{\pi I_0(1)}\exp(\cos 2\beta) \qquad \text{for} \quad 0 \leqslant \beta \leqslant \pi, \tag{25}$$

where I_0 is a modified Bessel function of order zero. This distribution is bimodal with

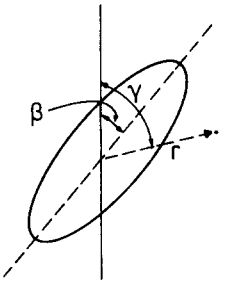

Figure 4. An ellipse whose major axis is inclined at an angle β to a fixed direction in an axisymmetric flow.

maximum values at $\beta = 0, \pi$ which are therefore preferred directions for L_2. A point with polar coordinates (r, γ) lies outside the ellipse on which $\Gamma = \theta$ if and only if $\gamma + (\pi/2) - \psi_0 \leqslant \beta \leqslant \gamma + (\pi/2) + \psi_0$. Thus

$$\mathbb{P}(\theta;\, r,\, \gamma,\, t) = \begin{cases} 1 & \text{for } \theta \geqslant \theta_{\max}; \\ \dfrac{1}{\pi I_0(1)} \displaystyle\int_{\gamma+\frac{\pi}{2}-\psi_0}^{\gamma+\frac{\pi}{2}+\psi_0} \exp(\cos 2\beta)\,\mathrm{d}\beta & \\ \quad \text{for } \theta_{\min} \leqslant \theta \leqslant \theta_{\max}; & \\ 0 & \text{for } \theta \leqslant \theta_{\min}. \end{cases} \tag{26}$$

Use of the rescaled variables defined in equation (20) then gives, by (16)

$$\pi I_0(1)\theta_{\max}\, p(\theta;\, r,\, \gamma,\, t) = \frac{\{\exp[-\cos 2(\gamma+\psi_0)] + \exp[-\cos 2(\gamma-\psi_0)]\}}{\Theta\left\{\ln\Theta\left(\ln\left[\dfrac{\Theta_{\min}}{\Theta}\right]\right)\right\}^{1/2}}. \tag{27}$$

The equivalent p.d.f. for an isotropic distribution of axes $p(\beta) = 1/(2\pi)$ is given by

$$\pi\theta_{\max}\, p(\theta;\, r,\, t) = \frac{\psi_0}{\Theta\left\{\ln\Theta\left(\ln\left[\dfrac{\Theta_{\min}}{\Theta}\right]\right)\right\}^{1/2}}. \tag{28}$$

Figure 5 shows the graphs of (27) (broken lines) and (28) (solid line) with $\Theta_{\min} = 0.01$ and with γ ranging from 0 (for points lying along the preferred direction) to $\pi/2$ (for points lying at right angles to it). It should be noted that both the curves (27) and (28) have a singularity near the values $\Theta = \Theta_{\min}$ and $\Theta = 1$. This is a result of the simple geometry in the flow with the *circle* radius r intersecting the ellipse at the ends of a *line* of length $2L_1$ and $2L_2$. The variation of p with γ is obvious; as γ increases to $\pi/2$, the point (r, γ) moves away from the most probable position of the ellipse with a subsequent increase in the probability of encountering lower concentrations and a decrease in p for higher concentrations. With this effect in mind, only the isotropic distribution of axes will be considered in the following section, since the effect of an axisymmetric distribution can be predicted.

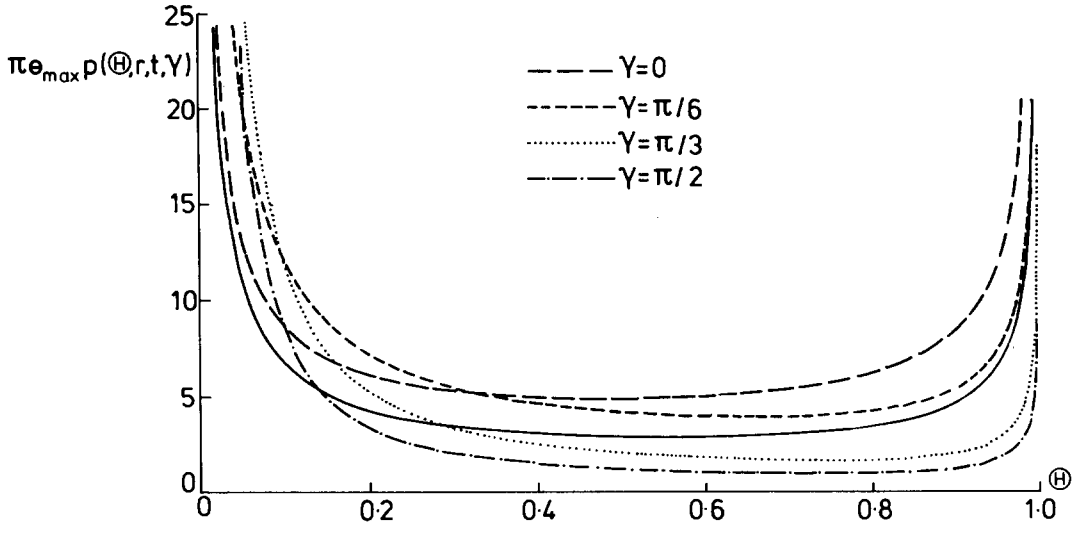

Figure 5. The broken lines show the p.d.f. given by equation (27) for a point (r, γ) in a two dimensional flow. The solid line is the corresponding isotropic distribution-equation (28).

4. Extensions of the simple models

The relatively simple exact solutions in Section 3 can be used to generate new solutions in many ways. For example the principal rates of strain can be regarded as random variables, and assigned probability distributions. Here two other extensions are discussed, each designed to incorporate other features of real turbulence and turbulent diffusion.

(i) The form of p must be determined in a framework which is fixed relative to some origin in the flow because most measurements of p are made in this way. P.d.f.s are therefore constructed for ensembles in which the centre of mass $|\bar{x}|$ is not fixed but moves randomly with a prescribed distribution $p(|\bar{x}|)$.

(ii) The number of ensembles in any one realization is not limited, as shown by careful inspection of the detailed structure in a real flow which is seen to be made up of several scalar spots at different stages of dispersion. A flow is examined containing several scalar clouds within each of which the concentration field is described by (11).

The variability of the position of the centre of mass of a cloud increases the complexity of the problem since the simple geometry that leads to relatively tractable results like (21) and (22) is destroyed. It is the expected probability $P(\theta; r, t\,||\,\bar{x}|)$ that the concentration at a point $r = |x|$ from a fixed origin is less than a value θ, given that the centre of the cloud is at a point $|\bar{x}|$, that must now be calculated. It follows that $\mathbb{P}(\theta; r, t)$ is then

$$\mathbb{P}(\theta; r, t) = \int_{|x|} P(\theta; r, t\,||\,\bar{x}|)\,p(|\bar{x}|)\,\mathrm{d}V(|\bar{x}|). \tag{29}$$

This procedure is perhaps best illustrated by considering the following concentration field

$$\Gamma(x, t) = A \exp\left\{-2\pi\left[\frac{(x_1 - |\bar{x}|)^2}{L_1^2} + \frac{x_2^2 + x_3^2}{L_3^2}\right]\right\}, \tag{30}$$

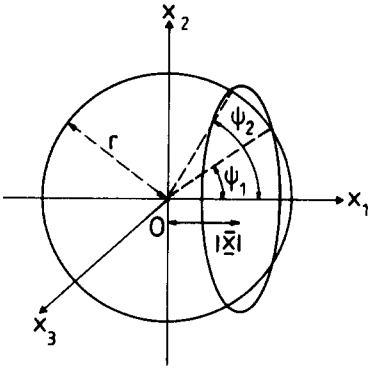

Figure 6. A discus whose centre of mass lies at a distance $|\bar{x}|$ from a fixed origin O intersecting a sphere radius r at points which subtend angles ψ_1, ψ_2 with the x_1 axis.

where $\alpha_2 = \alpha_3 > 0$, $\alpha_1 < 0$ – which corresponds to a discus whose centre is displaced a distance $|\bar{x}|$ from a fixed origin O along the positive x_1 axis; see Fig. 6. Following the procedure discussed in Section 3 we find $\Gamma = \theta$ when $\psi = \psi_1$ and when $\psi = \psi_2$, where the ψ satisfy

$$A \exp\left\{-2\pi\left[\frac{(r\cos\psi - |\bar{x}|)^2}{L_1^2} + \frac{r^2\sin^2\psi}{L_3^2}\right]\right\} = \theta. \tag{31}$$

For an isotropic distribution of L_1 and L_3, $P(\theta; r, t\,||\,\bar{x}|)$ is the portion of the surface area of a sphere radius r which lies outside the discus on which $\Gamma = \theta$ and is calculated from the values ψ_1 and ψ_2. It only remains to choose a function $p(|\bar{x}|)$ in order for $\mathbb{P}(\theta; r, t)$ to be found from (16) and (29). The detailed mathematics for several forms of $p(|\bar{x}|)$ is discussed in Kowe [19]. Here we give the results for the spherical normal distribution with

$$p(|\bar{x}|) = \frac{1}{(2\pi)^{3/2}\sigma^3}\exp\left\{-\frac{|\bar{x}|^2}{2\sigma^2}\right\} \qquad \text{for} \quad |\bar{x}| \geqslant 0, \tag{32}$$

where σ is a measure of the wandering of $|\bar{x}|$. Thus

$$p(\theta; r, t) = \begin{cases} \dfrac{L_1 L_3}{2(2\pi\sigma^2)^{3/2} r\theta}\displaystyle\int_{D_1 - r}^{D_1 + r} x^2 \,\mathrm{e}^{-x^2/(2\sigma^2)}\left\{x^2 - D_3^2\right\}^{1/2}\mathrm{d}x \\ \quad \text{for} \quad r \leqslant D_2; \\ \dfrac{L_1 L_3}{2(2\pi\sigma^2)^{3/2} r\theta}\left[\displaystyle\int_{r - D_1}^{D_1 + r} x^2 \,\mathrm{e}^{-x^2/(2\sigma^2)}\left\{x^2 - D_3^2\right\}^{1/2}\mathrm{d}x\right. \\ \quad \left. + 2\displaystyle\int_{D_3}^{r - D_1} x^2 \,\mathrm{e}^{-x^2/(2\sigma^2)}\left\{x^2 - D_3^2\right\}^{1/2}\mathrm{d}x\right] \\ \quad \text{for} \quad r \geqslant D_2. \end{cases} \tag{33}$$

where

$$D_1 = L_1\left\{\frac{1}{2\pi}\ln\left(\frac{A}{\theta}\right)\right\}^{1/2} \tag{34}$$

is the semi-minor axis of the discus on which $\Gamma = \theta$.

$$D_2 = L_3 D_1 / L_1, \tag{35}$$

is the semi-major axis, and

$$D_3 = \left[\frac{(L_3^2 - L_1^2)}{L_1^2}(r^2 - D_2^2)\right]^{1/2}. \tag{36}$$

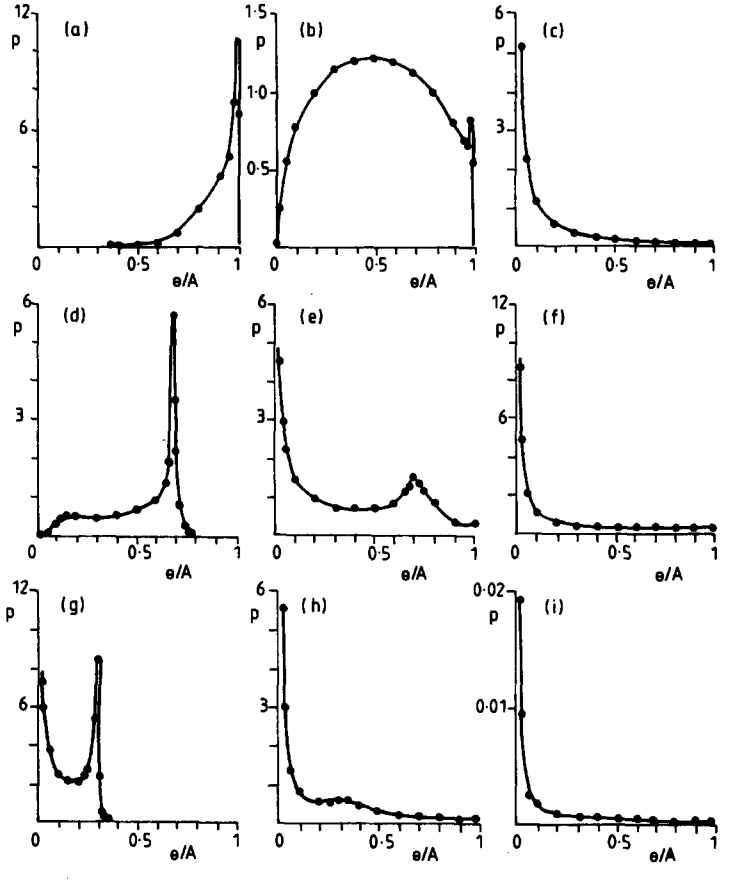

Figure 7. Some typical plots of $p(\theta; r, t)$ for a wandering discus, generated by varying the parameters r/L_1 and σ/L_1 in equation (33). (a), (b), (c) have $r/L_1 = 0.1$ with: (a) $\sigma/L_1 = 0.05\sqrt{2}$, (b) $\sigma/L_1 = 0.15\sqrt{2}$, (c) $\sigma/L_1 = 0.4\sqrt{2}$. (d), (e), (f) have $r/L_1 = 0.5$ with: (d) $\sigma/L_1 = 0.05\sqrt{2}$, (e) $\sigma/L_1 = 0.15\sqrt{2}$, (f) $\sigma/L_1 = 0.4\sqrt{2}$. (g), (h), (i) have $r/L_1 = 0.9$ with: (g) $\sigma/L_1 = 0.05\sqrt{2}$, (h) $\sigma/L_1 = 0.15\sqrt{2}$, (i) $\sigma/L_1 = 0.4\sqrt{2}$.

Figure 7 shows sketches of p defined in equation (33). The variation with r/L_1 and σ/L_1 is of prime interest; hence the variation with t is fixed by setting $L_3 = 2L_1$. The effect of r/L_1 on p can be seen in Figs. 7a, d., g. For small σ the discus is effectively fixed at the origin and we therefore expect p to have similar features to the plot in Fig. 2, i.e. an infinite spike near θ_{max} ($\Theta = 1$ in Fig. 2) and a smaller peak near θ_{min}, where θ_{max} and θ_{min} are defined by (13). When $r = 0.1L_1$, $\theta_{min} \approx \theta_{max}$ and the distribution appears to be one skewed spike. For intermediate values of r (Fig. 7d) θ_{max} and θ_{min} decrease since points on the surface of the sphere, radius r, intersect large ellipsoids of lower concentrations and the bimodality becomes more obvious. The spike at θ_{min} increases due to the decrease in the radius of curvature of the discus at the end of a line of length approximately $2L_1$, an effect which was noted in Section 3. As σ increases for a fixed value of r (see for example Figs. 7a, b, c) the distribution broadens as in Fig. 7b, since the range of concentration

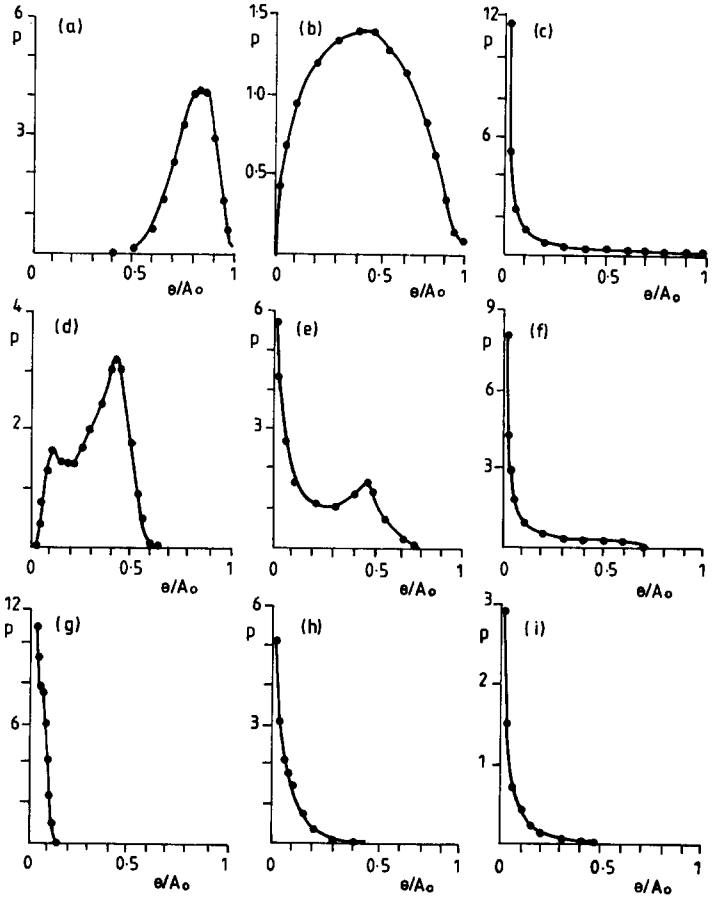

Figure 8. P.d.f.s for several wandering discuses obtained from equation (33) by allowing the maximum concentration A to vary with a truncated normal distribution – defined in the text. (a), (b), (c) have $r/L_1 = 0.1$, $\mu'/A_0 = 0.9$, $\sigma'/A_0 = 0.05\sqrt{2}$ with: (a) $\sigma/L_1 = 0.05\sqrt{2}$, (b) $\sigma/L_1 = 0.15\sqrt{2}$, (c) $\sigma/L_1 = 0.4\sqrt{2}$. (d), (e), (f) have $r/L_1 = 0.5$, $\mu'/A_0 = 0.68$, $\sigma'/A_0 = 0.05\sqrt{2}$ with: (d) $\sigma/L_1 = 0.05\sqrt{2}$, (e) $\sigma/L_1 = 0.15\sqrt{2}$, (f) $\sigma/L_1 = 0.4\sqrt{2}$. (g), (h), (i) have $r/L_1 = 0.8$, $\mu'/A_0 = 0.25$, $\sigma'/A_0 = 0.05\sqrt{2}$ with: (g) $\sigma/L_1 = 0.05\sqrt{2}$, (h) $\sigma/L_1 = 0.15\sqrt{2}$, (i) $\sigma/L_1 = 0.4\sqrt{2}$.

measured at a point r increases as the discus wanders across it. Eventually, for large values of σ, the point is most likely to lie in areas near zero concentration. This is reflected by the large spike near $\theta = 0$ in Fig. 7c.

The next step is to examine the effect of several scalar clouds in the same flow. It is unlikely in practice that each cloud will have the same time of dispersion so that the concentration A $(= A(t))$ will differ in each, having a maximum value $A_0 = 2^{3/2}Q/L_0^3$. The quantity A, therefore, can be regarded as a random variable in such a flow and is given a p.d.f. $p(A)$. Figure 8 shows the graphs of the p.d.f. for an ensemble of wandering discuses, given by integrating (33) over A, with $p(A)$ having the truncated normal distribution

$$p(A) = \left(\frac{2}{\pi}\right)^{1/2} \exp\left\{-\frac{(A-\mu')^2}{2\sigma'^2}\right\} \Big/ \sigma' \left\{\operatorname{erf}\left(\frac{A_0-\mu'}{\sigma'\sqrt{2}}\right) + \operatorname{erf}\left(\frac{\mu'}{\sigma'\sqrt{2}}\right)\right\}$$

$$\text{for } 0 \leqq A \leqq A_0, \tag{37}$$

where σ', μ' are constants. Full mathematical details of the formulation of p are given in Kowe [19].

It is interesting to compare the graphs in Fig. 8 with those in Fig. 7, which are drawn for the same values or r/L_1, σ/L_1, fixed σ'/A_0 and varying μ'/A_0. One immediate observation is that whilst the geometrical features of the p.d.f.s in Fig. 7 such as the bimodality are still in evidence, the plots in Fig. 8 are much smoother with sharp spikes becoming rounded, and in the case of the peak near $\theta_{\max}$ in Fig. 8b, disappearing altogether. This effect is due to the averaging process, and makes the plots in Fig. 8 qualitatively closer to measured values for p.

5. Discussion and conclusion

It has already been noted that in general the exact p.d.f.s derived in this paper are often very different from the standard p.d.f.s encountered in many elementary statistics courses; for example several of the graphs of $p(\theta; x, t)$ show bimodality. That measured p.d.f.s have, at least qualitatively, the same features is evident from Fig. 9 taken from [14], which shows $p(\theta; x, t)$ at four different radial positions in a particular cross-section of a methane jet entraining air. One principal motivation of the present work was to model the graphs in Fig. 9, and the results of this exercise are described in [21] and, in more detail, in [19].

Here it is more appropriate to emphasize a more general application of the results derived in this paper, and one of widespread potential importance for the mathematical modelling of engineering problems. As noted earlier, it is important in many situations to understand the behaviour of $p(\theta; x, t)$, and, ultimately, this will require knowledge of how to make acceptable approximations for the "non-closed" terms in (5). An indispensable tool in developing such approximations is to compare the results of different proposals with p.d.f.s obtained in other ways. In many respects the p.d.f.s obtained theoretically in the present paper are ideal for this validation procedure since they have been derived for simple flows and, especially in the case of the results of Section 3, they are exact.

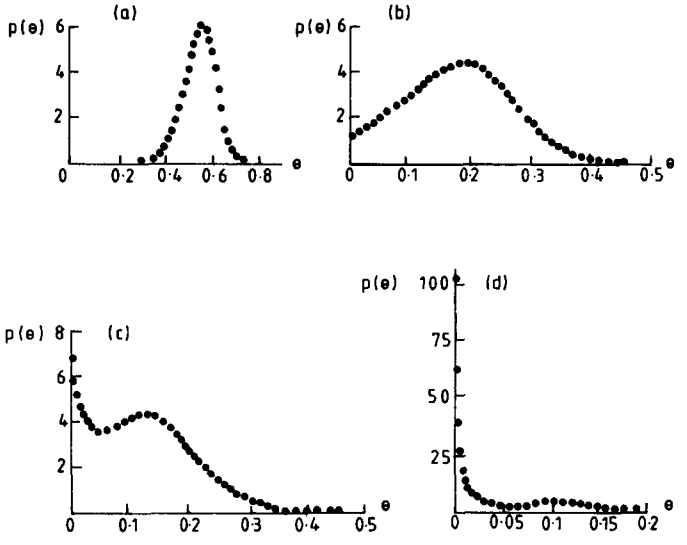

Figure 9. Measurements of $p(\theta; x, t)$ in a methane jet for several radial displacements r at a distance $10d$ downstream, where d is the jet diameter. The units are arbitrary. (a) $r/d = 0$, (b) $r/d = 1.3$, (c) $r/d = 1.5$, (d) $r/d = 1.8$.

Acknowldgements

R. Kowe is grateful for the financial support of SERC and British Gas during the period when this work was carried out, and both authors wish to thank Tony Birch, Colin Bradley, Roger Brown and Mike Dodson of the Midlands Research Station of British Gas for many interesting discussions.

References

[1] A.D. Birch, D.R. Brown and M.G. Dodson, Ignition probabilities in turbulent mixing flows, Report No. MRS E 374 (1980), Midlands Research Station, British Gas, Solihull, West Midlands, England.

[2] D.J. Ride, A probabilistic model for dosage, *Proc. IUTAM Symposium "Atmospheric Dispersion of Heavy Gases and Small Particles"*, (1984) Springer-Verlag, Berlin (G. Ooms and H. Tennekes, Eds.), 267–276.

[3] D.J. Ride, An assessment of the effects of fluctuations on the severity of poisoning by toxic vapours, *J. Haz. Mat.* 9 (1984) 235–240.

[4] P.C. Chatwin, The use of statistics in describing and predicting the effects of dispersing gas clouds, *J. Haz. Mat.* 6 (1982) 213–230.

[5] Z. Warhaft and J.L. Lumley, An experimental study of the decay of temperature fluctuations in grid-generated turbulence, *J. Fluid Mech.* 88 (1978) 659–684.

[6] P.C. Chatwin and P.J. Sullivan, Measurements of concentration fluctuations in relative turbulent diffusion, *J. Fluid Mech.* 94 (1979) 83–101.

[7] K.R. Sreenivasan, S. Tavoularis, R. Henry and S. Corrsin, Temperature fluctuations and scales in grid-generated turbulence, *J. Fluid Mech.* 100 (1980) 597–621.

[8] J.E. Fackrell and A.G. Robins, Concentration fluctuations and fluxes in plumes from point sources in a turbulent boundary layer, *J. Fluid Mech.* 117 (1982) 1–26.

[9] J.E. Fackrell and A.G. Robins, The effects of source size on concentration fluctuations in plumes, *Bound.-Layer Met.* 22 (1982) 335–350.

[10] P.C. Chatwin and P.J. Sullivan, The relative diffusion of a cloud of passive contaminant in incompressible turbulent flow, *J. Fluid Mech.* 91 (1979) 337–355.

[11] G.R. Newman, B.E. Launder and J.L. Lumley, Modelling the behaviour of homogeneous scalar turbulence, *J. Fluid Mech.* 111 (1981) 217–232.
[12] J.C. LaRue and P.A. Libby, Temperature fluctuations in the plane turbulent wake, *Phys. Fluids* 17 (1974) 1956–1957.
[13] R.A. Antonia, A. Prabhu and S.E. Stevenson, Conditionally sampled measurements in a heated turbulent jet, *J. Fluid Mech.* 72 (1975) 455–480.
[14] A.D. Birch, D.R. Brown, M.G. Dodson and J.R. Thomas, The turbulent concentration field of a methane jet, *J. Fluid Mech.* 88 (1978) 431–449.
[15] J. Janicka, W. Kolbe and W. Kollmann, Closure of the transport equation for the probability density function of turbulent scalar fields, *J. Non-Equil. Thermodyn.* 4 (1979) 47–66.
[16] S.B. Pope, The statistical theory of turbulent flames, *Phil. Trans. Roy. Soc.* A219 (1979) 529–568.
[17] P.G. Saffman, On the fine-scale structure of vector fields convected by turbulent fluid, *J. Fluid Mech.* 16 (1963) 545–572.
[18] A.A. Townsend, The diffusion of heat spots in isotropic turbulence, *Proc. Roy. Soc.* A 209 (1951) 418–430.
[19] R. Kowe, The probability density function of concentration in a turbulent shear flow, Ph. D. Thesis, University of Liverpool (1982).
[20] P.C. Chatwin and P.J. Sullivan, The structure of the probability density function of concentration in turbulent diffusion, Paper no. AIAA-80-1335, *Proc. 13th AIAA Fluid and Plasma Dynamics Conference*, Snowmass, Colorado (1980).
[21] R. Kowe and P.C. Chatwin, On modelling the probability density function of concentration in turbulent shear flows, *Proc. 8th Australasian Fluid Mechanics Conference*, Newcastle, NSW (1983), 3A.5–3A.8.